Application of the λ-Dynamics Method To Evaluate the Relative Binding Free Energies of Inhibitors to HCV Protease

Zhuyan Guo,* James Durkin, Thierry Fischmann, Richard Ingram, Andrew Prongay, Rumin Zhang, and Vincent Madison

Department of Structural Chemistry, Schering-Plough Research Institute, 2015 Galloping Hill Road, Kenilworth, New Jersey 07033

The λ-dynamics method was used to calculate the relative binding free energies of inhibitors to the hepatitis C virus (HCV) protease. A total of seven HCV protease p-side product inhibitors were used in this study. The inhibitors are 6-mer peptides spanning P6−P1 (Ac-Asp-D-Glu-Leu-Ile-Cha-P1-CO$_2$H). For this protein, S1 is a major hydrophobic pocket for binding. Binding of various residues to this pocket was investigated through free energy simulations and experimental inhibition constants. Several 300 ps λ-dynamics simulations in explicit solvent were performed. The relative binding free energy was estimated from these simulations. From a single simulation, the inhibitors can be correctly classified into highly potent and weakly potent groups. The multiple simulations give an accurate rank ordering of inhibitor potency; computed and experimental binding free energies agree with 0.6 kcal/mol for five of the seven inhibitors. In addition, free energy perturbation (FEP) calculations were carried out to validate the results from λ-dynamics. A total of 6 ligand pairs were compared. For each pair, 5−11 windows were used to map one ligand to the other. The cumulative simulation time was over 2 ns for each ligand pair. For four of the six ligand pairs, the λ-dynamics free energy difference fits better than the FEP difference to the experimental value. The fact that the λ-dynamics method achieved similar results in only a fraction of the total simulation time for FEP further demonstrates the robustness of the λ-dynamics method.

Introduction

Hepatitis C virus (HCV) is a major cause of non-A and non-B hepatitis, which can lead to mortality through either cirrhosis-induced hepatic failure or hepatocellular carcinoma. Currently, the only therapeutic regimens are subcutaneous interferon-α or PEG-interferon-α alone or in combination with oral ribavirin. The efficacy of the current therapeutics is moderate, which makes the need for new therapeutics highly desirable.[1]

Studies of HCV indicate that it is a positive-strand RNA virus of the flaviviridae family.[2] Its genome is translated into a polyprotein of ∼3000 amino acids in infected cells.[3−5] The HCV protease is located in the N-terminal domain of the NS3 protein. It is responsible for proteolytic cleavage at the NS3/NS4A, NS4A/NS4B, NS4B/NS5A, and NS5A/NS5B sites of the nonstructural region of the encoded polyprotein (Figure 1). Since the proteolytic processing steps in the HCV life cycle are required to produce infectious virus particles, its protease is a primary target for antiviral therapy.

Structure-based design plays a key role in the development of HCV protease inhibitors. The crystal structure of the HCV NS3 protease indicates that it is a serine protease with a trypsin/chymotrypsin-like fold.[6,7] Structures of the protease−inhibitor complex have also been reported.[8−10] These structures reveal that the inhibitors bind in an extended backbone conformation, forming an antiparallel β-sheet with one enzyme β-strand, as exemplified for a 6-mer peptide carboxylate
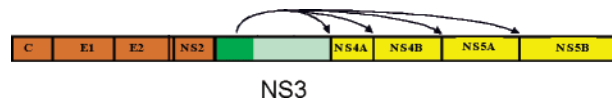

Figure 1. Schematic representation of the HCV polyprotein. NS3 is a bifunctional protein with protease and helicase activities. The green box represents the NS3 protease domain, and arrows depict cis and trans cleavages mediated by the NS3/NS4A protease complex.
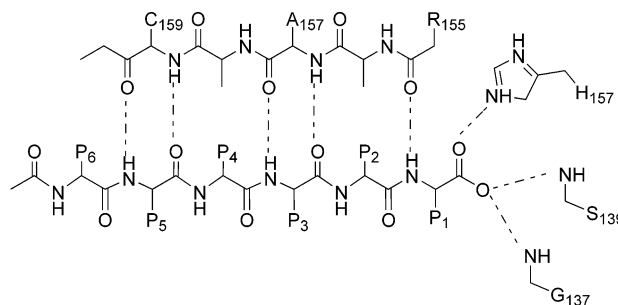

Figure 2. HCV protease inhibitors are bound through a combination of backbone hydrogen bonds and side chain hydrophobic interactions. P1, P3, and P5 residues make hydrogen bonds with an antiparallel β-strand of the protein. The terminal carboxylate oxygens bind to the oxyanion hole (Ser139, Gly137) and to the catalytic His57.

acid inhibitor in Figure 2. The P1 residue contributes most to the binding energy, whereas the rest of the side chains are at least partially solvent-exposed. Although the S1 pocket is the largest and most important hydrophobic pocket for inhibitor binding, it is actually rather small compared with the active site pockets of many other enzymes. Because of the lack of a significant

* To whom correspondence should be addressed. Phone: 908-740-3796. Fax: 908-740-4640. E-mail: zhuyan.guo@spcorp.com.
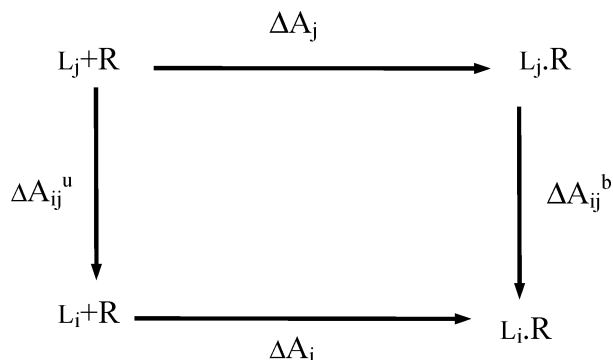
Figure 3. Schematic representation of the thermodynamic cycle. L_i is the ith ligand. R is the protein receptor. $L_i + R$ and $L_i \cdot R$ represent ligand and the protein in the unbound and bound states, respectively. ΔA_i is the free energy of binding of ligand i. ΔA_{ij}^u and ΔA_{ij}^b are the free energy change of mutation from ligand j to ligand i in the unbound and bound states, respectively.

binding pocket, the design of HCV protease inhibitors is challenging. So far, most of the HCV protease inhibitors developed have been peptide-based and utilize the backbone hydrogen-bonding network.

As an integral part in the design of new therapeutics, computational approaches that rapidly evaluate relative binding free energies of ligands could play an important role in identifying and optimizing inhibitors. The development of efficient and accurate free energy based computational methods has been an area of active research. Although free energy perturbation (FEP) and thermodynamic integration (TI) methods are rather accurate and well established,[11,12] they are too slow to be of practical use in drug design. Multiple simulations have to be performed to map one inhibitor to the other in order to obtain the free energy difference. To balance the demand for speed and accuracy, the λ-dynamics method for ligand binding free energy calculations has been developed recently.[13–16] Within a short simulation time, this method partitions the inhibitors into good binders and poor binders. Longer simulation times yield a (semi)quantitative measure of the relative binding free energy of multiple ligands.

In this work, the λ-dynamics method was used to study the relative binding free energies of HCV protease inhibitors. The results were compared with experimental data. To further validate application of the λ-dynamics method to this system, FEP calculations were performed. Reasonably good agreement was obtained between the two theoretical methods as well as between theoretical and experimental results.

Materials and Methods

Theory. In a typical experiment, the free energy difference between two ligands is obtained from $\Delta \Delta A_{ij} = \Delta A_i - \Delta A_j$, where ΔA_i and ΔA_j are the binding free energies of ligands i and j, respectively. Since free energy is a function of state only, the thermodynamic cycle depicted in Figure 3 translates the calculation of $\Delta \Delta A_{ij}$ into the free energy changes for mutation from ligands j to i in both the unbound (ΔA^u) and the bound (ΔA^b) states. That is,

$$\Delta \Delta A_{ij} = \Delta A_i - \Delta A_j = \Delta A_{ij}^b - \Delta A_{ij}^u \qquad (1)$$

This is the basis for the well-established FEP method.[12] In a FEP calculation, only two ligands can be evaluated at a time.

One is considered as the reactant, the other is considered as the product. A coupling coefficient λ ($0 < \lambda < 1$) is used to map the reactant to the product. To overcome the sampling problems, several simulations with different values of λ have to be performed. The free energy changes for all the λ intervals are added together to obtain the overall free energy change.

The λ-dynamics method is an extension of the FEP method, but instead of pairwise comparison, multiple ligands are evaluated simultaneously within a single λ-dynamics calculation. To perform a λ-dynamics calculation, a hybrid potential is constructed for a set of L chemically distinct species:

$$V(\{\lambda\},(x)) = \sum_{i=1}^{L} \lambda_i^2 (V_i(x) - F_i) + V_{env}(x) \qquad (2)$$

where

$$\sum_{i=1}^{L} \lambda_i^2 = 1$$

As in the FEP method, $V_{env}(x)$ is the interaction involving only the environmental atoms (e.g., solvent, protein, and the part of the molecule that is invariant among all the ligands), $V_i(x)$ is the interaction involving any of the atoms in the distinct part of molecule i, and λ_i is the coupling parameter for ligand i. F_i is the biasing potential. In ligand binding free energy calculations, it corresponds to the free energy of a ligand in the unbound state. The value of F_i needs to be determined prior to the λ-dynamics calculation. Note that there is no interaction among atoms in distinct groups; i.e., ligands are invisible to one another. Unlike standard FEP, each λ_i is treated as a volumeless fictitious particle with mass m_i and evolves to "find" the low free energy regions of the λ-space as the system fluctuates. The dynamics of the system is governed by the extended Hamiltonian.[17,18]

$$H(\{\lambda\},(x)) = T_x + T_\lambda + \sum_{i=1}^{L} \lambda_i^2 (V_i(x) - F_i) + V_{env}(x) \quad (3)$$

Here, T_x and T_λ are the kinetic energy of the atomic coordinates and the λ variables, respectively. From the partition function of the hybrid system,

$$Z(\{\lambda\},x) = \int \exp\left(-\frac{1}{k_b T}(\sum_{i=1}^{L} \lambda_i^2 (V_i(x) - F_i)) + V_{env}(x)\right) dx \qquad (4)$$

the free energy difference between any two molecules i and j can be calculated from

$$\Delta \Delta A_{ij} = -k_b T \ln \frac{P_i(\lambda_i=1,\{\lambda_{k\neq i}\}=0)}{P_j(\lambda_j=1,\{\lambda_{l\neq j}\}=0)} \qquad (5)$$

where $P(\lambda_i=1,\lambda_{k\neq i}=0)$ is the probability that the hybrid system is in a state dominated by inhibitor i. Therefore, from the probability distribution of states having $\lambda_i^2 = 1$ and $\lambda_j^2 = 1$, the difference in free energy between the two molecules can be obtained.

Force Field Parameters and Simulation Details. The force field parameters for standard protein residues are available in Quanta CHARMM.[19] For nonstandard P1 residues, the atomic charges assigned were consistent with the charges of comparable standard residues.

The X-ray structure of the protein−inhibitor complex provided the initial coordinates. A hybrid ligand, which encompassed the original ligand (P1 = Cys) and all the variant groups, was constructed. The missing coordinates of the hybrid ligand and hydrogen atoms were built using CHARMM.[20] The system is centered at the hybrid ligand. A cap of TIP3P waters was added to fill the space in a 24 Å sphere.[21] Residues outside

the sphere were deleted. The final system contains 112 protein residues, 40 crystal waters, and 1262 bulk waters.

The X-ray structures of protease−inhibitor complexes indicate that there is no notable movement of the active site upon inhibitor binding except for a few flexible side chains. Therefore, harmonic restraints were imposed on selected atoms to prevent unrealistic movement during long dynamics simulations. For residues that are more than 6 Å away from the inhibitor atoms, a harmonic restraint with a force constant of 20 kcal/(mol·Å²) was applied to both the side chain and backbone heavy atoms of the protein (no mass weighting was used). A force constant of 5 kcal/(mol·Å²) was applied to the protein backbone atoms within 6 Å of the inhibitor. No restraint was imposed on those side chains that have at least one atom within 6 Å of the inhibitor heavy atoms.
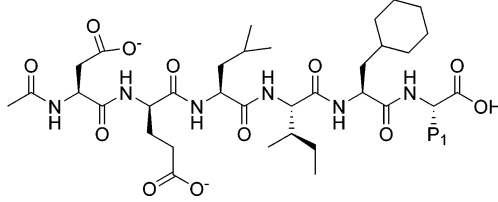
λ-Dynamics simulations of the solvated protein−ligand complex were carried out using CHARMM. A total of six simulations were performed, three include all seven inhibitors and three include Mcy, Ecy, Hcy, and Nle. All the simulations started with different initial conditions. For each set of three simulations, the initial coordinates were obtained by minimizing the system for 100, 500, and 1000 steps and random velocities following the Gaussion distribution were assigned. During the dynamics simulations, the system temperature was maintained at 300 K. The velocities were reassigned every 200 steps using a Gaussion distribution if the temperature during this period was outside the target 300 ± 5 K. Bonds involving hydrogen atoms were constrained using the SHAKE algorithm.[22] The time step of the simulation was 1.5 fs. A cutoff of 11 Å was used for nonbond interactions (electrostatic and van der Waals). A solvent boundary force was used to retain the water molecules.[23] The masses of the λ variables were chosen to be 20 amu·Å², which is comparable to the mass of a carbon atom. The system was equilibrated for 45 ps followed by 300 ps of data collection. The value of each λ was recorded every 10 time steps.

FEP calculations were carried out using the same solvated protein−ligand system. For each pairwise transformation, 5−11 windows, each with fixed λ value between 0 and 1, were used to map the reactant to the product. For each λ, 45 ps of equilibration was followed by 300 ps of data collection. The free energy change within each λ interval was less than $2kT$ (~1.2 kcal/mol). In addition, FEP calculations of the unbound ligands in explicit solvent were performed in order to calculate the free energy of the unbound ligand in solution, namely, F_i in eq 2 or ΔA^u in Figure 3. Note that the incorporation of F_i into the Hamiltonian of eq 2 ensures that the resulting free energy from the λ-dynamics simulation corresponds to the binding free energy of the ligands. Without this term, the result would be the free energy of the ligands in the bound state, which is only half of the thermodynamic cycle.

Results and Discussion

The Inhibitors. Seven HCV protease p-side product inhibitors were used in this study. They are 6-mer peptides spanning P6−P1 (Ac-Asp-D-Glu-Leu-Ile-Cha-P1-CO₂H). The crystal structure of the NS3 protease complexed with NS4A and the inhibitor (P1 = Cys) was solved at 2.5 Å resolution.[10] As illustrated in Figure 2, the inhibitor binds through a combination of backbone hydrogen bonds and side chain hydrophobic interactions. The C-terminal carboxylate oxygens make hydrogen bonds to the oxyanion hole and His 57, respectively. The binding constants, K_i, of the inhibitors and their chemical structures are given in Table 1. The inhibitors vary only at the P1 position. The K_i values of these inhibitors range from 0.12 to 80 μM. Therefore, the binding free energy difference between the most (Cys) and the least (Hcy) potent inhibitors is about 4.0 kcal/mol. The experimental uncertainty is 3-fold, or 0.7 kcal/mol.

Table 1. Chemical Structure and Binding Data for the HCV Protease Inhibitors[a]

name	P1	K_i (μM)
Cys	CH_2SH	0.12
Nva	$(CH_2)_2CH_3$	0.13
Mcy	CH_2SCH_3	0.5
Abu	CH_2CH_3	0.6
Nle	$(CH_2)_3CH_3$	2.0
Ecy	$CH_2SCH_2CH_3$	5.0
Hcy	$(CH_2)_2SH$	80.0

[a] P1 is the site of substitution. A hybrid residue is built that contains all the substitutions at P1. The inhibitors share the rest of the inhibitor atoms called the common atoms.
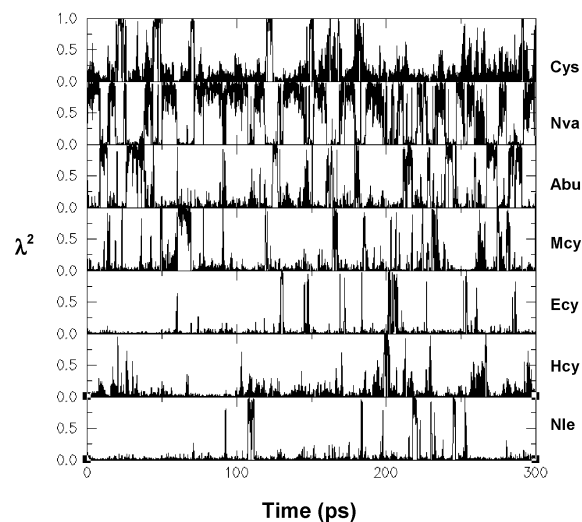

Figure 4. Example of the λ-dynamics trajectory of seven inhibitors during a 300 ps simulation. The names of the inhibitors are shown on the right.

Ranking the Inhibitors via λ-Dynamics. According to eq 5, the free energy difference between ligands can be calculated from the ratio of the probabilities of the two ligands having $\lambda^2 = 1$. In a λ-dynamics calculation, P_i corresponds to the fraction of time that ligand i has $\lambda_i^2 = 1$. Therefore, a good estimate of binding free energy requires sufficient sampling of the λ parameter in the $\lambda^2 = 1$ state. It is noteworthy that at any instant only one ligand may have $\lambda^2 = 1$, which is guaranteed by the constraint in eq 2. For visualization, Figure 4 plots the trajectory of the λ parameter for one of the simulations involving all seven inhibitors. In this plot, Cys, Nva, Abu, and Mcy frequently reached the $\lambda^2 \approx 1$ state over the course of simulation. Therefore, these four are predicted to be the more potent inhibitors and their λ parameters are sampled well enough to give relative binding free energies. Ecy, Hcy, and Nle have values of λ near 1 sampled less frequently. This second set of inhibitors is predicted to be less potent, but their λ parameters are not sufficiently sampled to give reliable binding energies.

It is interesting to note that a 300 ps simulation was able to sample all the inhibitors, thereby providing an

Table 2. Predicted Relative Binding Free Energies ($\Delta\Delta A$) from λ-Dynamics Calculations Compared with Experimental Values[a]

| P1 residue | F_i | $\Delta\Delta A$ (kcal/mol) | | |
		λ-dynamics	experiment	difference of $\Delta\Delta A$
Cys	0.0	0.0	0.0	0.0
Nva	0.4	-0.5 ± 0.3	0.1	-0.6
Mcy	0.6	0.5 ± 0.2	0.9	-0.4
Abu	-0.9	-0.1 ± 0.1	1.0	-1.1
Nle	-1.8	2.0 ± 0.7	1.7	0.3
Ecy	0.8	1.6 ± 0.6	2.2	-0.6
Hcy	-5.1	2.2 ± 0.8	3.9	-1.7

[a] The "difference of $\Delta\Delta A$" is the result from λ-dynamics minus experiment. Cys is the reference inhibitor. The values of F_i from FEP calculations are also listed. The experimental error is 0.7 kcal/mol.

initial estimate of the relative binding free energies of the inhibitors from a single simulation. This is in contrast to the FEP method in which several simulations have to be performed with different λ values between 0 and 1 before any estimate of the relative binding free energy of any two inhibitors could be obtained. Besides its efficiency, the λ-dynamics method is also more flexible because additional simulations can be performed and the results can be combined to improve the prediction. Two additional 300 ps λ-dynamics simulations involving all seven inhibitors and a second set of three 300 ps simulations involving Mcy, Ecy, Hcy, and Nle were performed to improve the estimates of the binding free energies and to obtain additional sampling of the weakly bond inhibitors. Here, Mcy is included in the simulations as the reference for the weaker inhibitors, putting the two sets on the same energy scale. We feel that running multiple simulations may be more efficient than a single long simulation because kinetic trapping, as often occurs in dynamics simulations, can be avoided and all the simulations can be run simultaneously. Comparing the separate simulations gives an estimate of the statistical error.

From each simulation, an estimate of the ligand binding free energy was obtained according to eq 5 using the approximation that the inhibitor "i" is favored for all time segments when $\lambda_i^2 \geq 0.9$. The results from all the separate simulations were averaged to give the mean binding free energy along with the average deviation from the mean, as shown in Table 2. The corresponding experimental values are also listed. The method clearly identified Cys, Nva, Mcy, and Abu as more potent than Nle, Ecy, and Hcy. The relatively small average deviation for Cys, Nva, Mcy, and Abu reflects the fact that these inhibitors are well sampled during each simulation. For all the inhibitors except Abu and Hcy, the predicted binding free energies are within 0.6 kcal/mol of the observed values and are

within the combined experimental and sampling errors. Larger discrepancies occurred for Abu (1.1 kcal/mol) and Hcy (1.7 kcal/mol), which exceed the combined errors of 0.8 and 1.5 kcal/mol, respectively. Besides sampling, other causes of error may be (1) the force field parameters and (2) the estimation of the free energy of the inhibitor in the unbound state, i.e., F_i in eq 2.

FEP Calculations. As an established free energy calculation method, FEP calculations were carried out to validate the λ-dynamics results. Since both the λ-dynamics and the FEP calculations in this study used the same force field and simulation specifications, errors caused by the force field could be eliminated when the results from the two methods are compared. Also, since both calculations used the same reference state for the unbound inhibitors, i.e., F_i in Table 2 for the λ-dynamics calculations and ΔA^u in Table 3 for the FEP calculations, errors from the estimation of F_i (or ΔA^u) also can be ruled out in the comparison of the ligand binding free energies. With a total of seven inhibitors, six pairwise transformations were required for the FEP calculations. They are (Cys → Nva), (Nva → Abu), (Hcy → Ecy), (Mcy → Abu), (Nle → Ecy), and (Ecy → Mcy). For each pair, the ligand with the larger volume was defined as the reactant and was mapped to the product ligand through a series of simulations. The changes of binding free energy ($\Delta\Delta A$) in mapping one ligand to the other are summarized in Table 3. Here, ΔA^b and ΔA^u indicate the free energy change of ligands in the bound and unbound states, respectively. The corresponding values for the λ-dynamics method were derived from Table 2. Overall, the calculations are consistent with each other. The pairwise differences between the two methods range from 0.1 to 0.6 kcal/mol.

Although the focus of the FEP calculations was to validate the results from λ-dynamics, it is interesting to note that the results from both methods also compare well with experimental results. The experimental value for each ligand pair is listed in the last column of Table 3. For the FEP simulations, the pairs (Cys → Nva), (Nle → Ecy), and (Ecy → Mcy) match experimental values within 0.6 kcal/mol. For the remaining three pairs, namely, (Nva → Abu), (Hcy → Ecy), and (Mcy → Abu), the difference from the experimental results is about 1 kcal/mol. For two of these pairs, the λ-dynamics simulations better match the experimental results (within 0.5 kcal/mol). In fact, the λ-dynamics values are closer to the experimental values for four out of six pairs and all but one pair match the experimental values within 0.6 kcal/mol.

In the discussion of the λ-dynamics results (Table 2), we noted that the prediction for the inhibitor Hcy differs from the experimental value by 1.7 kcal/mol. In the

Table 3. Comparison of the λ-Dynamics Calculations with FEP[a]

| reactant → product | FEP | | | λ-dynamics | experiment |
	ΔA^u (kcal/mol)	ΔA^b (kcal/mol)	$\Delta\Delta A$ (kcal/mol)	$\Delta\Delta A$ (kcal/mol)	$\Delta\Delta A$ (kcal/mol)
$\Delta\Delta A$ (Cys → Nva)	0.4	0.5	0.1	-0.5	0.1
$\Delta\Delta A$ (Nva → Abu)	-1.3	-1.5	-0.2	0.4	0.9
$\Delta\Delta A$ (Hcy → Ecy)	5.9	5.4	-0.5	-0.6	-1.7
$\Delta\Delta A$ (Mcy → Abu)	-1.5	-2.6	-1.1	-0.6	-0.1
$\Delta\Delta A$ (Nle → Ecy)	2.6	2.1	-0.5	-0.4	-0.5
$\Delta\Delta A$ (Ecy → Mcy)	-0.2	-1.2	-1.0	-1.1	-1.3

[a] The corresponding experimental values are also listed. ΔA^u and ΔA^b are the free energy change of the ligands in the unbound and bound states, respectively. The change in binding free energy is calculated from $\Delta\Delta A = \Delta A^b - \Delta A^u$.

pairwise comparison involving Hcy, namely, (Hcy → Ecy) in Table 3, the difference from experiment is about 1 kcal/mol for both methods. This discrepancy may arise from systematic errors in the force field.

Conclusions

The λ-dynamics method described above for ligand binding free energy calculations is conceptually very similar to competitive binding experiments carried out in the laboratory in that multiple ligands simultaneously compete for the same common receptor based on their relative binding free energies. When the ratio of bound to free ligand concentrations in solution is determined, the relative binding affinity of ligands can be inferred. Thus, a "best" ligand can be selected accordingly. Similarly, by determining the relative population of each $\lambda_i^2 \approx 1$, one can distinguish favorable binders from unfavorable ones and estimate the relative binding free energies of the favorable ones. The method can be used to evaluate compounds with modifications either at a single site or at multiple sites. The strength of the method is its ability to evaluate a large number of compounds simultaneously without increasing the computational time significantly, because only one solvated protein is needed for the simulation despite multiple inhibitors.

The λ-dynamics method has proven to be successful in applications to small rigid molecules (e.g., imidazole analogues) where modifications at various sites are made or in perturbations that are confined to a single site such as in this work. The protocol used in this study should be applicable for the study of other peptide inhibitors. More work needs to be done to assess the applicability of the method to different systems.

The λ-dynamics method is much more efficient than FEP. In this work, the cumulative simulation time used in the λ-dynamics calculations is about the same as that for a FEP transformation for one pair of ligands. In other words, the λ-dynamics method achieved similar results in less than 20% of the total simulation time used in FEP.

Supporting Information Available: Partial atomic charges of nonstandard amino acids. This material is available free of charge via the Internet at http://pubs.acs.org.

References

(1) Houghton, M. Hepatitis C viruses. In *Fields Virology*, 3rd ed.; Fields, B. N., Knipe, D. M., Howley, P. M., Eds.; Lippincott-Raven Publishers: Philadelphia, PA, 1996; pp 1035−1058.

(2) Choo, Q. L.; Kuo, G.; Weiner, A. J.; Overby, L. R.; Bradley, D. W.; et al. Isolation of a cDNA clone derived from a blood-borne non-A, non-B viral hepatitis genome. *Science* **1989**, *244*, 359−362.

(3) Kato, N.; Hijikata, M.; Ootsuyama, Y.; Nakagawa, M.; Ohkoshi, S.; et al. Molecular cloning of the human hepatitis C virus genome from Japanese patients with non-A, non-B hepatitis. *Proc. Natl. Acad. Sci. U.S.A.* **1990**, *87*, 9524−9528.

(4) Choo, Q. L.; Richman, K. H.; Han, J. H.; Berger, K.; Lee, C.; et al. Genetic organization and diversity of the hepatitis C virus. *Proc. Natl. Acad. Sci. U.S.A.* **1991**, *88*, 2451−2455.

(5) Takamizawa, A.; Mori, C.; Fuke, I.; Manabe, S.; Murakami, S.; et al. Structure and organization of the hepatitis C virus genome isolated from human carriers. *J. Virol.* **1991**, *65*, 1105−1113.

(6) Love, R. A.; Parge, H. E.; Wickersham, J. A.; Hostomsky, Z.; Habuka, N.; et al. The crystal structure of hepatitis C virus NS3 proteinase reveals a trypsin-like fold and a structural zinc binding site. *Cell* **1996**, *87*, 331−342.

(7) Kim, J. L.; Morgenstern, K. A.; Lin, C.; Fox, T.; Dwyer, M. D.; et al. Crystal structure of the hepatitis C virus NS3 protease domain complexed with a synthetic NS4A cofactor peptide. *Cell* **1996**, *87*, 343−355.

(8) Barbato, G.; Cicero, D. O.; Cordier, F.; Narjes, F.; Gerlach, B.; et al. Inhibitor binding induces active site stabilization of the HCV NS3 protein serine protease domain. *EMBO J.* **2000**, *19*, 1195−1206.

(9) Marco, S. D.; Rizzi, M.; Volpari, C.; Walsh, M. A.; Narjes, F.; et al. Inhibition of the hepatitis C virus NS3/4A protease. *J. Biol. Chem.* **2000**, *275*, 7152−7157.

(10) Prongay, A.; et al. Unpublished results.

(11) Beveridge, D. L.; DiCapua, F. M. Free energy via molecular simulation: Applications to chemical and biomolecular systems. *Annu. Rev. Biophys. Biophys. Chem.* **1989**, *18*, 431−492.

(12) Kollman, P. Free energy calculations: Application to chemical and biochemical phenomena. *Chem. Rev.* **1993**, *93*, 2395−2417.

(13) Kong, X.; Brooks, C. L., III. λ-Dynamics: A new approach to free energy calculations. *J. Chem. Phys.* **1996**, *105*, 2414−2423.

(14) Guo, Z.; Brooks, C. L., III. Rapid screening of binding affinities: Application of the λ-dynamics method to a trypsin-inhibitor system. *J. Am. Chem. Soc.* **1998**, *120*, 1920−1921.

(15) Guo, Z.; Brooks, C. L., III; Kong, X. Efficient and flexible algorithm for free energy calculations using the λ-dynamics approach. *J. Phys. Chem. B* **1998**, *102*, 2032−2036.

(16) Banba, S.; Guo, Z.; Brooks, C. L., III. New free energy based methods for ligand binding from detailed structure−function to multiple-ligand screening. In *Free Energy Calculations in Rational Drug Design*; Reddy, M. R., Erion, M. D., Eds.; Kluwer Academic/Plenum Publishers: New York, 2001.

(17) Nose, S. A unified formulation of the constant temperature molecular dynamics methods. *J. Chem. Phys.* **1984**, *81*, 511−519.

(18) Ji, J.; Cagin, T.; Pettitt, B. M. Dynamics simulations of water at constant chemical potential. *J. Chem. Phys.* **1992**, *96*, 1333−1342.

(19) Momany, F.; Rone, R. Validation of the general purpose QUANTA 3.2/CHARMM force field. *J. Comput. Chem.* **1992**, *13*, 888−900.

(20) Brooks, B. R.; Bruccoleri, R. E.; Olafson, B. D.; States, D. J.; Swaminathan, S.; et al. CHARMM: A program for macromolecular energy, minimization, and dynamics calculations. *J. Comput. Chem.* **1983**, *4*, 187−217.

(21) Jorgensen, W. L.; Chandraseklar, J.; Madura, J. D.; Impey, R. W.; Klein, M. L. Comparison of simple potential functions for simulating liquid water. *J. Chem. Phys.* **1983**, *79*, 926−935.

(22) Ryckaert, J. P.; Ciccotti, G.; Berendsen, H. J. C. Numerical integration of the Cartesian equations of motion of a system with constraints: Molecular dynamics of *n*-alkanes. *J. Comput. Phys.* **1977**, *23*, 327−341.

(23) Brooks, C. L., III; Karplus, M. Deformable stochastic boundaries in molecular dynamics. *J. Chem. Phys.* **1983**, *79*, 6312−6325.

JM030040O